



## **Return value estimates of significant wave height along Bulgarian Black Sea coast**

**Neyko M. Neykov\*, Vasko Galabov, Anna Kortcheva, Plamen N. Neytchev**

*National Institute of Meteorology and Hydrology- BAS,  
Tsarigradsko shose 66, 1784 Sofia, Bulgaria*

**Abstract:** The classical monthly block maxima approach in extreme value analysis is adapted for the estimation of the return values of significant wave ( $H_s$ ) heights hindcast data at the open-sea locations near Shabla, Emine and Ahtopol stations in the western Black Sea. The hindcast data consists of 3 hourly generated data by the Simulating Waves Nearshore (SWAN) model covering the period of 111 years (1901–2010). The ERA-CLIM wind fields produced by the European Center for Medium-Range Weather Forecasts (ECMWF) are used to force the SWAN model. The standard and profile likelihood return values are computed for several return periods and compared with previously estimated return values based on visual observations.

**Keywords:** return level, significant wave height, generalized extreme value distribution, Black Sea, SWAN model, wave hindcast, ERA-CLIM.

---

### **1. INTRODUCTION**

Information on extreme wave climate is of vital importance for coastal and marine activities. Estimates of the  $m$ -year return value of significant wave height are needed for the safety control, design of ship, offshore, and coastal structures, and for the mapping of flood risk areas. Such information is very important for the implementation of the EU Floods Directive (FD 2008/60/EC) for development of flood hazard maps for vulnerable zones along the Bulgarian Black Sea coast (Dimitrov et al., 2013) and flood risk management. Unfortunately, such information is scarce for the western part of the Black sea. Wave climate at selected points along the Bulgarian Black Sea coast is investigated in Grozdev (2008) and Dimitrov et al. (2013) based on the visual wave observations obtained from the NIMH-BAS weather stations network. The visual observations

---

\* neyko.neykov@meteo.bg

are subjective and must be calibrated with measurements. However, a comparison between visual observations and available instrumental wave measurements has not been performed at these studies. Furthermore, according to the World Meteorological Organization (WMO), wave heights are assessed in an ordinal scale and reported in standard sea state codes as Table 1. For example, sea state code 6 means the waves are in range between 4 and 6 meters. This adds an additional uncertainty for the statistical analyses.

**Table 1.** WMO Sea State Code.

Code	Wave height	Characteristics
0	0 metres	Calm (glassy)
1	0 to 0.1 metres	Calm (rippled)
2	0.1 to 0.5 metres	Smooth (wavelets)
3	0.5 to 1.25 metres	Slight
4	1.25 to 2.5 metres	Moderate
5	2.5 to 4 metres	Rough
6	4 to 6 metres	Very rough
7	6 to 9 metres	High
8	9 to 14 metres	Very high
9	Over 14 metres	Phenomenal

The goal of this study is to estimate the return values of significant wave ( $H_s$ ) heights hindcast data at the open-sea locations Shabla, Emine and Ahtopol in the Bulgarian Black Sea region. The  $H_s$  is employed as a basic parameter describing the sea state. It is defined as the average height of the one-third part of the measured waves having the largest wave heights at a given location. The location of the point Shabla is  $43.60^\circ\text{N}$ ;  $28.90^\circ\text{E}$ , the location of the point Emine is  $42.70^\circ\text{N}$ ;  $28.20^\circ\text{E}$  and the location of the point Ahtopol is  $42.20^\circ$ ;  $28.20^\circ\text{E}$ .

The paper is organized as follows. Section 2 describes the wave hindcast data sets and performs exploratory data analysis, Section 3 shortly reviews the classical extreme value methodology, Section 4 describes the extreme value methodology application to  $H_s$  hindcast data, discusses the obtained findings and results. Conclusions are made in Section 5.

## 2. WAVE HINDCAST AND EXPLORATORY DATA ANALYSIS

Historical series of  $H_s$  data in this study are based on a long-term numerical hindcast using the SWAN wave model (Booij et al, 1999). The  $H_s$  is defined as the average height of the highest one third wave amplitudes at a given location. The SWAN model is one of the state-of-art third generation wave models. The model is successfully implemented

in the Black Sea (Akpınar et al, 2012; Rusu and Ivan, 2010) and used to study the Black Sea wave climate (Valchev et al, 2010; Arkhipkin et al., 2014; Akpınar et al. 2016; Galabov et al. 2012; Galabov et al. 2013; Galabov et al. 2015a; Galabov et al. 2015b). Atmospheric forcing for the wave model- the 10m wind data is derived from the atmospheric reanalysis ERA-CLIM (ERA 20CM dataset) (Stickler et al. 2014). ERA-CLIM is an European reanalysis of global climate observations for the XX century using recovered and digitized data of early meteorological observations. The spatial resolution of the reanalysis is close to 1 degree and the temporal resolution is 3 hours. The reanalysis is based only on surface observations in order to avoid artificial trends caused by the increasing amounts of assimilated data. We use the ERA-Clim data from July 1901 to June 2010 in order to have the entire winter seasons included in the hindcast. More details about ERA-CLIM can be found in Stickler et al. (2014).

The computational domain of SWAN is based on a regular spherical grid covering the entire Black Sea with a spatial mesh size of  $0.0333^\circ$ . The version of SWAN used in the study is 40.91.ABC. We use the default parameterizations of the physical processes in SWAN in order to keep the results comparable with other studies. More details are given in Galabov et al. (2012) and Galabov (2014). The most important parameterizations of the wave generation by wind and wave dissipation by whitecapping are based on the scheme of Komen (Komen et al. 1984) with the tuning parameter in the whitecapping parameterization changed from 0 to 1 known as “Rogers trick” (Rogers et al. 2003).

The long-term model simulations are split in one year model runs for the period 1901-2010 and each run is initialized by the previous run last computation. The model output data sets for three selected locations are stored at 3-hour intervals. The output points are situated near to the coastal weather station of NIMH-BAS in the town of Ahtopol and Emine and Shabla capes. The selected points are at 50m water depth in order to ensure that it satisfies the deep water condition (depth that is more than half of the wave length even for significant storms). In this way we eliminate the influence of the finite water depth mechanisms of wave energy dissipation. The obtained return periods in deep water may be later transferred to the intermediate and shallow water running SWAN with very high spatial resolution and data about the bottom slope to simulate the wave transformation.

The choice of these locations is based on the fact that they are representative for the northernmost part of the Bulgarian coast, the middle part of the coast between the bays of Varna and Burgas and for the Southern Bulgarian coast.

## **2.1. Exploratory Hs data analysis**

In order to get an impression of Hs data some standard plots are discussed. Figure 1 shows a portion of 3 hourly Hs series from the hindcast, obtained in meters at Ahtopol (left) and Shabla (right). It is evident that the data exhibits strong annual cycle. In particular, the winter Hs data has quite different characteristics in comparison with the

summer one. On the plots of Figures 2 and 3 three types of  $H_s$  box plots about Ahtopol and Shabla are given in order to show the wave datasets distribution in different time scales.

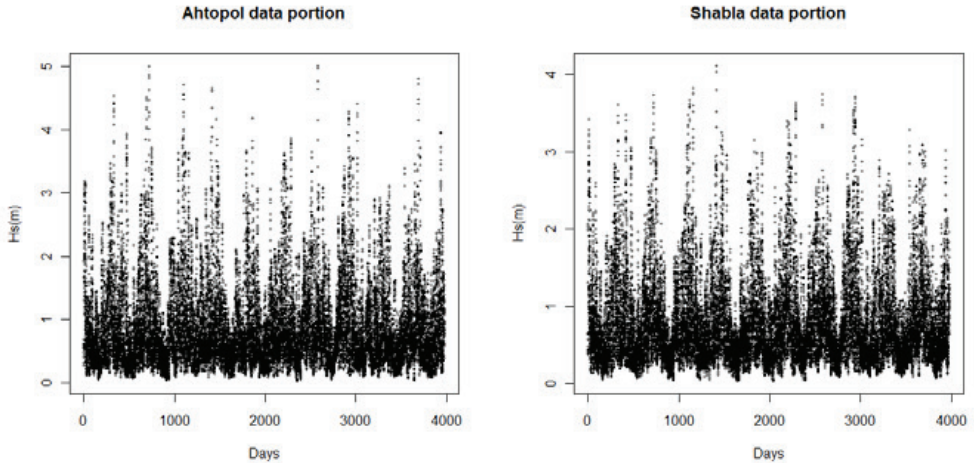


**Fig. 1.** Portion of Ahtopol (left) and Shabla (right)  $H_s$  data set.

One can see the variation from year to year concerning the upper tail of the data at the upper panels of these plots. The remaining panels of these figures show the variation in  $H_s$  data with season and time of day.  $H_s$  data exhibits strong annual cyclical patterns according to the middle panel plots. It is evident that waves are higher during the cold half of the year from October to March. However, no pattern can be identified in diurnal variation.

### 3. STATISTICAL METHODOLOGY OF EXTREMES

Key results in extreme value theory according to Coles (2001), Embrechts et al. (1997), and Reiss and Thomas (2001) point to the generalized extreme value (GEV) distribution as a model for block maxima of independent observations, with distribution function:

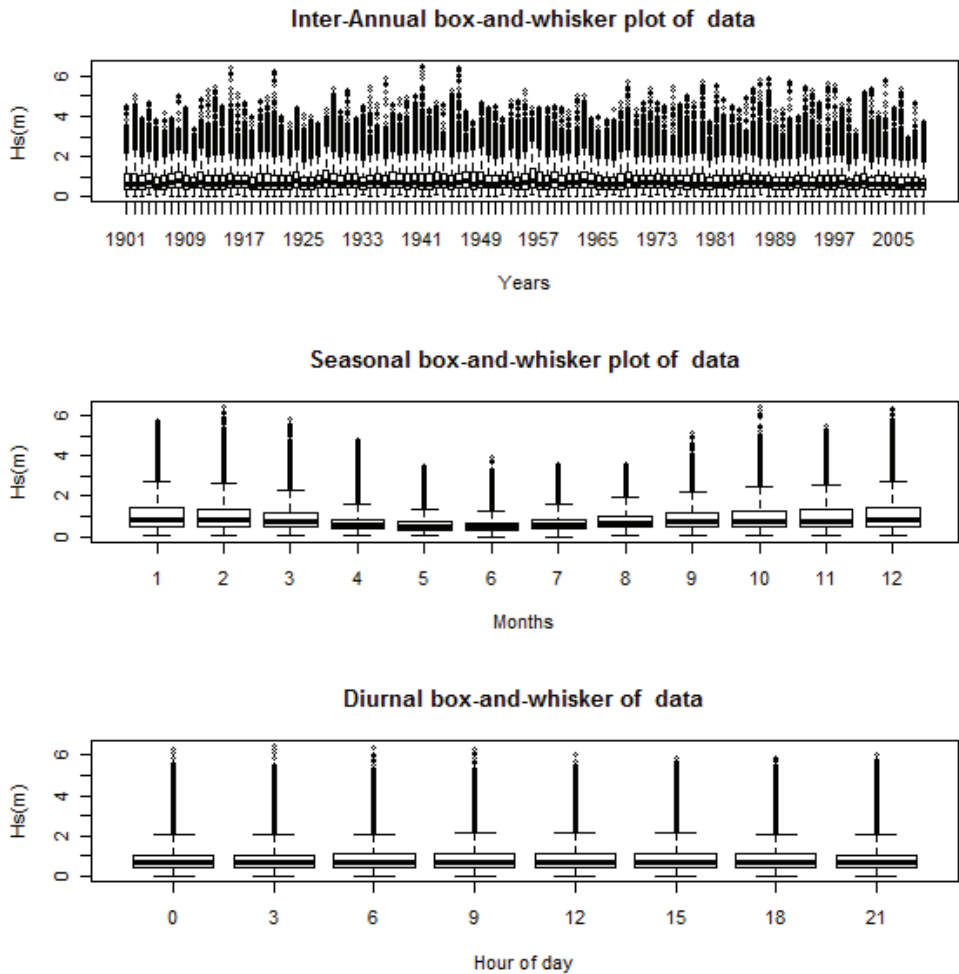
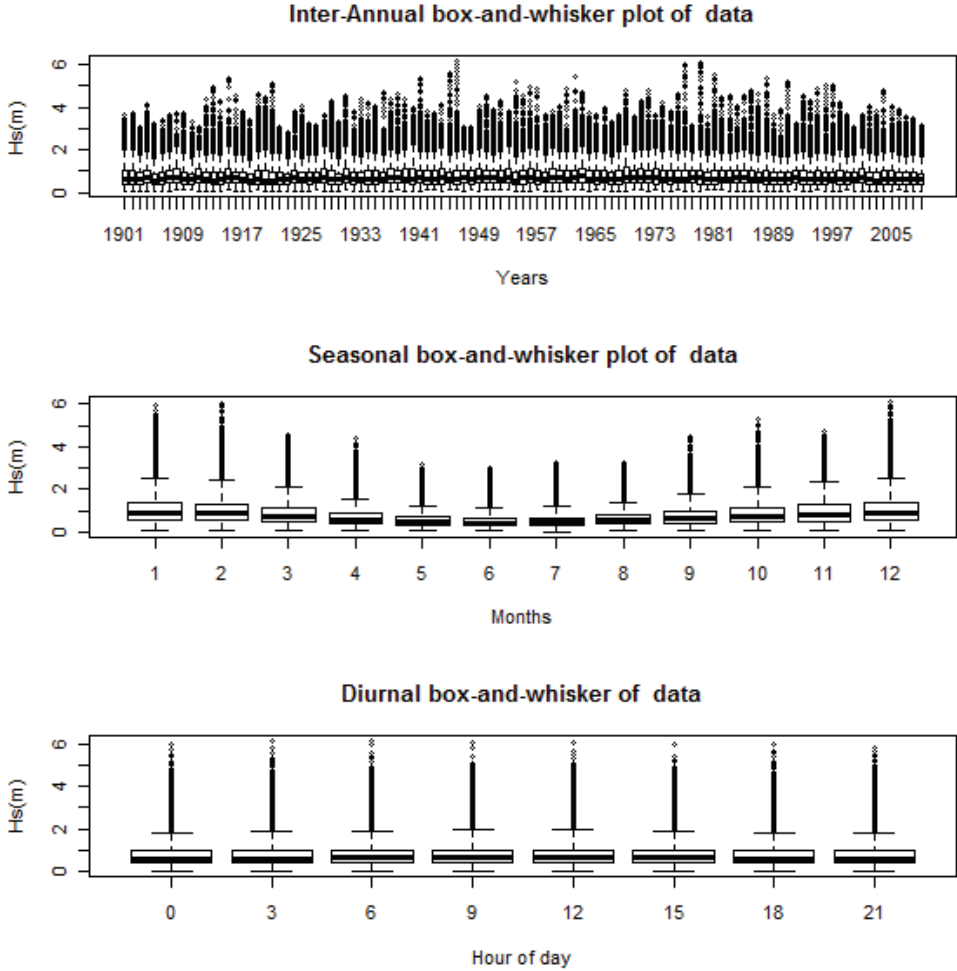


Fig. 2. Ahtopol: Inter-annual, seasonal and diurnal variation of Hs data for the period 1901-2010.



**Fig. 3.** Shabla: Inter-annual, seasonal and diurnal variation of Hs data for the period 1901-2010.

$$G(z) = \begin{cases} \exp \left\{ - \left[ 1 + \xi \left( \frac{z-\mu}{\sigma} \right) \right]^{-\frac{1}{\xi}} \right\}, & \xi \neq 0 \\ \exp \left\{ - \exp \left[ \frac{z-\mu}{\sigma} \right] \right\}, & \xi = 0 \end{cases} \quad (1)$$

defined on  $\{z: 1 + \xi(z - \mu)/\sigma > 0\}$ , where  $-\infty < \mu < \infty$ ,  $\sigma > 0$ , and  $-\infty < \xi < \infty$  are location, scale and shape parameters, respectively and the case  $\xi = 0$  is taken to be the limit as  $\xi \rightarrow 0$ . The location parameter  $\mu$  indicates the center of the distribution, the

scale parameter  $\sigma > 0$  indicates the spread of the distribution, and the shape parameter  $\xi$  indicates the behavior of the distribution's upper tail. Based on the shape parameter value, the GEV encompasses the classical three types of distributions: the Gumbel, Fréchet, and Weibull. The Gumbel class of distributions is defined for  $\xi = 0$ . This class is characterized by an unbounded light-tailed which decreases relatively rapidly as exponential decay. The Fréchet class is a heavy-tailed distribution with  $\xi > 0$  which is characterized with relatively slower decreasing tail rate. The Weibull class of distributions is obtained for  $\xi < 0$ . The distributions of this class are short-tailed distributions with finite upper bounds. The upper and lower points, i.e., the end-points of GEV distributions equal  $\mu - \sigma/\xi$  for  $\xi < 0$  and  $\xi > 0$  respectively.

By setting  $G(z_p) = 1 - p$  for  $0 < p < 1$ , the  $(1 - p)$ -quantile for the GEV distribution is obtained by inversion of the GEV distribution function,  $G^{-1}(1 - p)$  which leads to the formula

$$z_p = \begin{cases} \mu - \frac{\sigma}{\xi} [1 - \{-\log(1 - p)\}^{-\xi}], & \xi \neq 0 \\ \mu - \sigma \log\{-\log(1 - p)\} & \xi = 0. \end{cases} \quad (2)$$

In common terminology  $z_p$  is the return level associated with the return period of  $1/p$  years, i.e., level exceeded on average once every  $1/p$  years. More precisely, it is the level  $z_p$  exceeded by the annual maximum in any year with probability  $p$ . Loosely, the  $z_p$  return level is the value that could be expected to occur once in  $1/p$  years under a stationary climate that excludes the effect of future climate change. Thus, long return periods correspond to small  $p$  values, i.e. 10, 100, 1000 and 5000 year periods correspond to 0.1, 0.01, 0.001 and 0.0002.

Using the block maxima  $z_1, \dots, z_m$ , the unknown parameters of the GEV model can be estimated by maximizing the log-likelihood function

$$l(\mu, \sigma, \xi) = -m \log \sigma \left(1 + \frac{1}{\xi}\right) \sum_{i=1}^m \log \left[1 + \xi \left(\frac{z_i - \mu}{\sigma}\right)\right] + \sum_{i=1}^m \left[1 + \xi \left(\frac{z_i - \mu}{\sigma}\right)\right]^{-\frac{1}{\xi}} \quad (3)$$

under the constraint  $\{z_i: 1 + \xi(z_i - \mu)/\sigma > 0\}$  for  $i=1, \dots, m$ .

We note that on an annual scale the block maxima  $z_i$  for  $i = 1, \dots, m$  are the maxima among 365(366) observations whereas for monthly scale each block consist of 28 (29) observations for February and 30 or 31 observations for the remaining months of the year.

Let  $\hat{\mu}$ ,  $\hat{\sigma}$  and  $\hat{\xi}$  be the maximum likelihood estimates (MLE) of the unknown GEV parameters  $\mu$ ,  $\sigma$  and  $\xi$ . Their standard confidence intervals can be constructed using the

diagonal elements of the estimated variance-covariance matrix  $V(\theta) = \left(-\frac{\partial^2 l(\theta)}{\partial \theta_i \partial \theta_j}\right)^{-1}$

evaluated at  $\hat{\theta} = (\hat{\mu}, \hat{\sigma}, \hat{\xi})$ . The return level estimate  $\hat{z}_p$  for  $0 < p < 1$  can be obtained by substituting  $\hat{\mu}$ ,  $\hat{\sigma}$  and  $\hat{\xi}$  into (2) whereas the return level confidence intervals of  $\hat{z}_p$  can be constructed using the standard delta method

$$\text{Var}(\bar{z}_p) \simeq \nabla z_p^T V(\theta) \nabla z_p$$

where the gradient  $\nabla z_p^T = \left( \frac{\partial z_p}{\partial \mu}, \frac{\partial z_p}{\partial \sigma}, \frac{\partial z_p}{\partial \xi} \right)$  and  $V(\theta)$  are evaluated at  $\hat{\theta}$ .

The profile likelihood estimates and the corresponding confidence intervals of the above parameters are preferable because the MLE normal approximation can be poor in case of small  $m$ . For instance, the profile likelihood estimate of the return level  $z_p$  can be obtained by replacing

$$\mu = z_p + \frac{\sigma}{\xi} [1 - \{-\log(1 - p)\}^{-\xi}]$$

into (3) and maximizing the likelihood function  $l(z_p, \sigma, \xi)$  on the new set of parameters. In a similar way profile likelihood estimate for  $\sigma$  and  $\xi$  can be obtained.

Standard quality fit can be checked via diagnostic plots. For instance, the probability (PP) plot plots the points  $(\tilde{G}(z_{(i)}), \hat{G}(z_{(i)}))$  for  $i = 1, \dots, m$  where  $z_{(1)} \leq \dots \leq z_{(m)}$  are the ordered block maxima and

$$\tilde{G}(z_{(i)}) = \frac{i}{m+1} \text{ and } \hat{G}(z_{(i)}) = \exp \left\{ - \left[ 1 + \hat{\xi} \left( \frac{z_{(i)} - \hat{\mu}}{\hat{\sigma}} \right) \right]^{-\frac{1}{\hat{\xi}}} \right\}.$$

The points should follow the line  $\mathbf{y} = \mathbf{x}$  provided the GEV distribution is reasonable. The quantile (QQ) plot is defined as the inverse of the PP plot and plots the points

$$\left\{ \left( z_{(i)}, \hat{G}^{-1} \left( \frac{i}{m+1} \right) \right) = \left( z_{(i)}, \hat{\mu} - \frac{\hat{\sigma}}{\hat{\xi}} \left[ 1 - \left\{ -\log \left( \frac{i}{m+1} \right) \right\}^{-\hat{\xi}} \right] \right) \right\}, \quad i = 1, \dots, m.$$

Departure from linearity in the PP and QQ plots is a fit failure indication.

#### 4. HS DATA ANALYSIS

Typically, the extremes are analyzed on an annual time scale. However, because of the strong non-stationary behavior of Hs data we chose the block monthly maxima model resulting in a sample size of  $n=110$  for the period 1901-2010 for each month of the year. We can afford this due to the medium sample size, which help to justify the use of the MLE. Maximization of the GEV log-likelihood (3) for Ahtopol February Hs data leads to the estimate  $(\hat{\mu}, \hat{\sigma}, \hat{\xi}) = (2.9416, 0.8687, -0.0603)$  for which the negative

log-likelihood value is 153.6231. The estimates, their 95% lower and upper confidence intervals denoted by LCI and UCI and the approximate variance-covariance matrix are presented in Table 2. The diagonals of the variance-covariance matrix correspond to the variances of the individual parameter of  $(\hat{\mu}, \hat{\sigma}, \hat{\xi})$ . The corresponding standard errors of the estimates are obtained by taking the square roots of the diagonal elements. The results given in Table 3 and 4 are about Emine and Shabla for annual January maxima of Hs data.

**Table 2.** Ahtopol parameter estimates, 95% confidence intervals and approximate variance-covariance matrix for February block maxima of Hs data.

Location Ahtopol				Appr. variance-covariance matrix		
Parameter	95% LCI	Estimate	95% UCI	location $\mu$	scale $\sigma$	shape $\xi$
location $\mu$	2.7546	2.9416	3.1285	0.0048	0.0004	-0.0016
scale $\sigma$	0.7322	0.8687	1.0052	0.0004	0.0023	-0.0014
shape $\xi$	-0.2204	-0.0603	0.0998	-0.0016	-0.0014	0.0039
shape-profile $\xi$	-0.2097	-0.0600	0.1055			

**Table 3.** Shabla parameter estimates, 95% confidence intervals and approximate variance-covariance matrix for January block maxima of Hs data.

Location Shabla				Appr. variance-covariance matrix		
parameter	95% LCI	Estimate	95% UCI	location $\mu$	scale $\sigma$	shape $\xi$
location $\mu$	2.7080	2.8438	2.9796	0.0048	0.0012	-0.0017
scale $\sigma$	0.5465	0.6444	0.7422	0.0012	0.0025	-0.0010
shape $\xi$	-0.1536	-0.0180	0.1175	-0.0017	0.0010	0.0048
shape-profile $\xi$	-0.1410	-0.0180	0.1289			

**Table 4.** Emine parameter estimates, 95% confidence intervals and approximate variance-covariance matrix for January block maxima of Hs data.

Location Emine				Appr. variance-covariance matrix		
parameter	95% LCI	Estimate	95% UCI	location $\mu$	scale $\sigma$	shape $\xi$
location $\mu$	2.7929	2.9379	3.0829	0.0055	0.0014	-0.0023
scale $\sigma$	0.5699	0.6756	0.7814	0.0014	0.0029	-0.0017
shape $\xi$	-0.2019	-0.0471	0.1077	-0.0023	-0.0017	0.0062
shape-profile $\xi$	-0.2103	-0.0479	0.1128			

The MLE of  $\xi$  is negative for Ahtopol, Emine and Shabla and thus corresponds to a Weibull bounded distribution. Their estimated upper end-points  $\hat{\mu} - \hat{\sigma}/\hat{\xi}$  of the

distribution are 17.34m, 17.28m and 38.59m, respectively. On the other hand, the 95% confidence interval extends above zero, so that the strength of evidence from the data for a bounded distribution is not strong.

The plots on Fig. 4 show the profile log-likelihood for  $\xi$  based on Ahtopol (left) and Shabla (right) Hs data. The standard estimate and shape-profile estimates are given in Tables 2-4, from which 95% confidence intervals for  $\xi$  are obtained. The delta method assumes that the parameter estimates are symmetric, which is typically not the case for the shape parameter of GEV distribution. The vertical gray dashed line of the plots points out the maximum of the log likelihood at the shape estimate  $\hat{\xi}$ . The shape profile confidence interval is obtained as projection of the intersection points of the blue horizontal line, the 95% quantile of the  $\chi_1^2$  distribution, with log-likelihood function onto the horizontal axis, see the left and right vertical dashed blue lines. These shape profile confidence intervals are only slightly different to the confidence intervals based on standard MLE asymptotic results but clearly there is an asymmetry.

The return periods and their return levels based on delta method and profile likelihood are given in Tables 5-7. It is seen that delta method and profile likelihood return levels differ. This is because of the profile log-likelihood surface asymmetry, the extent of which increases with increasing return period. The profile log-likelihoods for the 100 and 5000-years return levels for Ahtopol and Shabla data are shown on the left and right plots of Figure 5. The vertical gray dashed line of the plots points out the maximum of the log likelihood at  $\hat{z}_p$  - the return level estimate. The profile confidence interval of  $\hat{z}_p$  is obtained as projection of the points of intersection of the horizontal line, the 95% quantile of the  $\chi_1^2$  distribution, with log-likelihood function onto the horizontal axis; see the left and right vertical dashed blue lines. It can be seen from both Tables 5-7 and Figure 5 that the return levels for Hs increase for longer period of time. Clearly, there is strong asymmetry that has to be expected as the higher waves variation is much larger than the lower. This means that not only the GEV distribution location parameter but the scale parameter as well is important for statistical modeling purposes of non-stationary time series Hs data.

The standard graphical diagnostics including probability and quantile plots indicate suitable fits for the block maxima according to the plots shown in Fig. 6 and 7 for Shabla and Emine Hs data. The lower left plots are about the GEV density fit to Hs data whereas the lower right plots are about the return levels. The tiny circles on the return level plots represent  $\hat{z}_p$  on the vertical axis against  $(-\log(1-p))$  on the horizontal axis on a logarithmic scale,  $(\log(-\log(1-p)), \hat{z}_p)$ , for specified return periods, the solid black line is the GEV model fit to the Hs data whereas the blue lines are the associated 95% confidence intervals estimated by the delta method. It is seen that the return level curve provide a satisfactory representation of the empirical estimates although the confidence intervals are wider for long return periods. Consequently, all four diagnostic plots lend support to the quality of the fitted GEV model. Diagnostics plots of similar quality but not presented in the paper are obtained for Ahtopol Hs data as well.

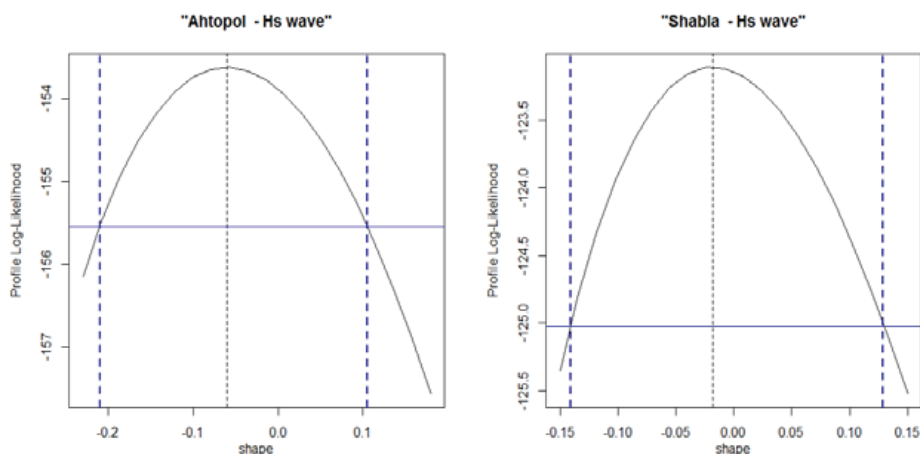


**Fig. 4.** Profile likelihood shape estimate for in Ahtopol (February) and Shabla (January) Hs data.

**Table 5.** Ahtopol - return periods and levels based on February block maxima of Hs data.

return period (years)	return levels - delta method			return levels - profile likelihood		
	95% LCI	Estimate	95% UCI	95% LCI	Estimate	95% UCI
10	4.41	4.77	5.13	4.46	4.77	5.22
50	5.16	5.96	6.76	5.39	5.96	7.13
100	5.36	6.43	7.50	5.70	6.43	8.06
500	5.59	7.44	9.30	6.26	7.44	10.47
1000	5.60	7.85	10.10	6.44	7.85	11.65
5000	5.46	8.73	11.99	6.93	8.73	14.72

**Table 6.** Shabla - return periods and levels based on January block maxima of Hs data.

return period (years)	return levels - delta method			return levels - profile likelihood		
	95% LCI	Estimate	95% UCI	95% LCI	Estimate	95% UCI
10	3.98	4.26	4.55	4.01	4.27	4.62
50	4.65	5.27	5.89	4.81	5.27	6.18
100	4.85	5.69	6.53	5.10	5.69	6.96
500	5.16	6.63	8.10	5.65	6.63	9.03
1000	5.22	7.03	8.83	5.87	7.03	10.09
5000	5.23	7.93	10.63	6.34	7.93	12.71

**Table 7.** Emine - return periods and levels based on January block maxima of Hs data.

return periods (years)	return levels - delta method			return levels - profile likelihood		
	95% LCI	Estimate	95% UCI	95% LCI	Estimate	95% UCI
10	4.09	4.38	4.67	4.13	4.38	4.74
50	4.71	5.35	5.98	4.89	5.35	6.30
100	4.88	5.73	6.59	5.14	5.73	7.07
500	5.09	6.58	8.07	5.62	6.58	9.12
1000	5.11	6.92	8.74	5.79	6.92	10.14
5000	5.02	7.68	10.34	6.12	7.68	12.81

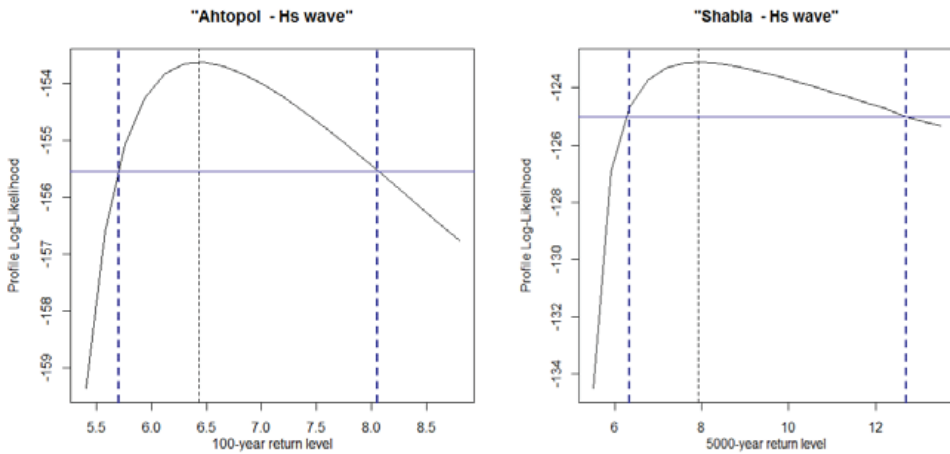


**Fig. 5.** Profile log-likelihood for 100 and 5000-year return levels in the Ahtopol and Shabla Hs data.

The probabilities of exceeding various thresholds of interest can be calculated once the parameters of the GEV model have been estimated using Hs data. For instance, the risks of occurrence of Hs greater than 6m, 7m and 7.4m for Ahtopol are 0.037201, 0.000345 and 0.000029 whereas for Shabla are 0.014506, 0.000848 and 0.000204, respectively.

The package ismev ported in R by Stephenson (2002) is used to perform the computations and plots of the paper.

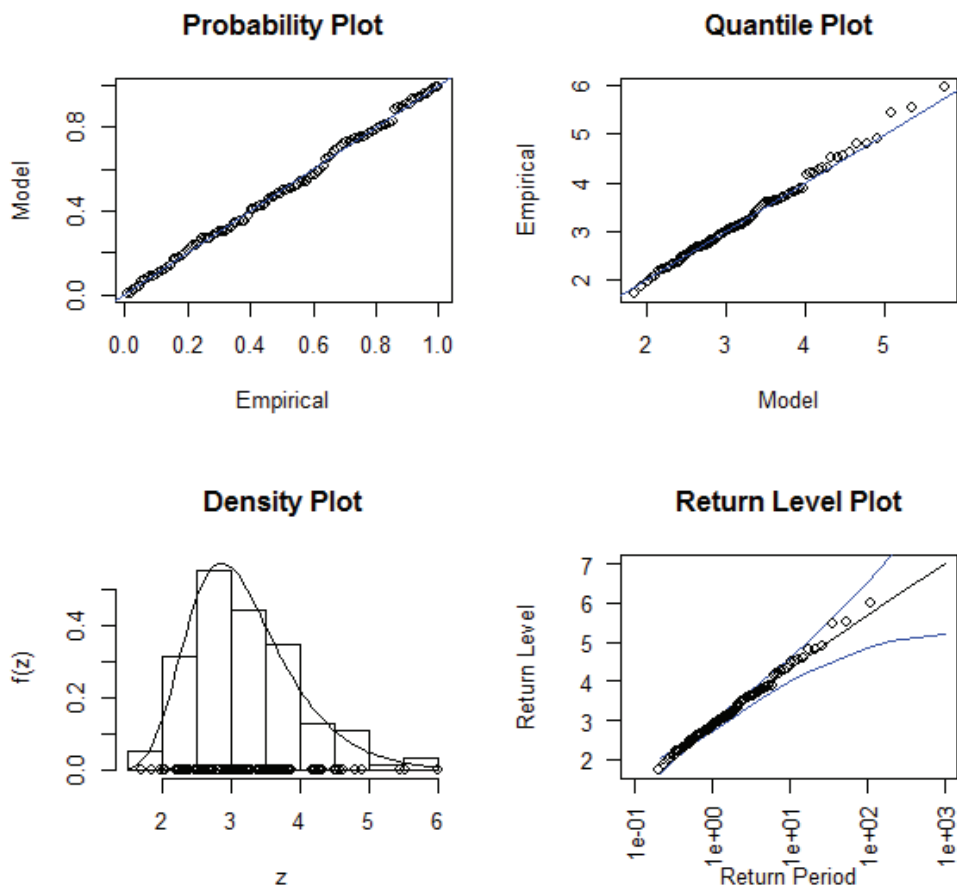


Fig. 6. Diagnostic plots for GEV fit to the Shabla (January) Hs data.

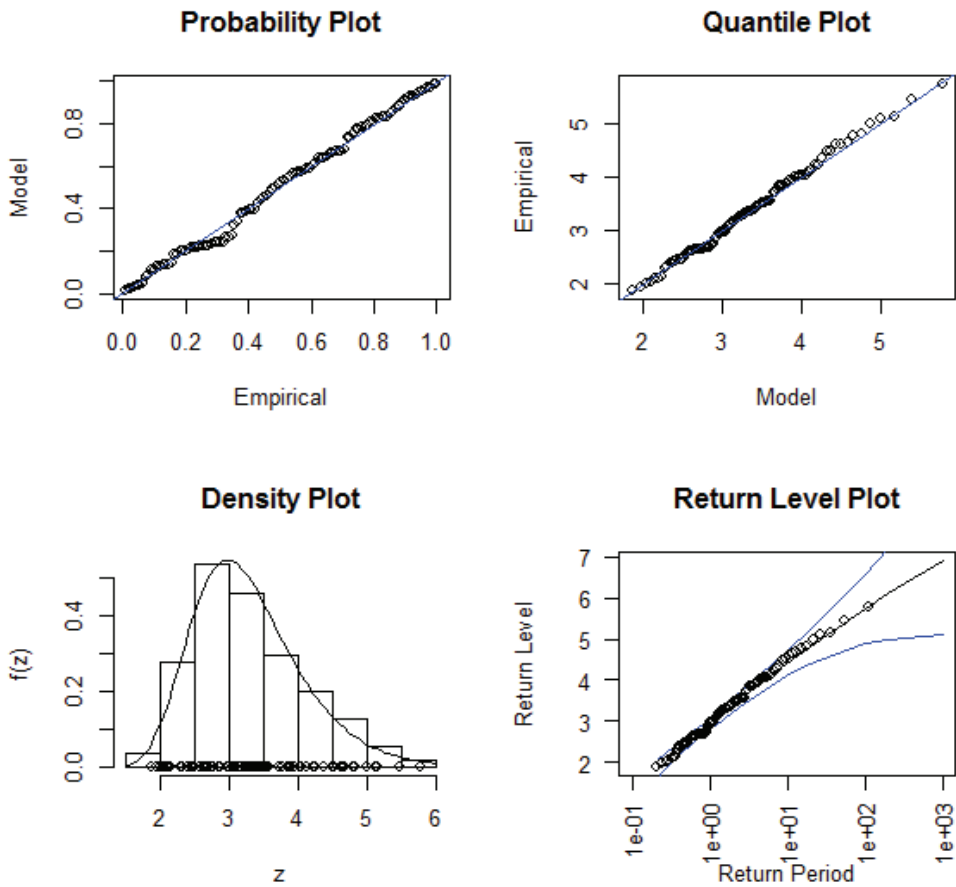


Fig. 7. Diagnostic plots for GEV fit to the Emine (January) Hs data.

## 5. DISCUSSION AND CONCLUSIONS

The Hs monthly return values are estimated for different return periods using hindcast data at the open-sea locations Ahtopol, Emine and Shabla within the Bulgarian Black Sea region. The uncertainty in these return values is quantified by the standard delta method and profile confidence interval of 95% level. As a whole, the estimated return values at these locations are lower in comparison with those reported by Grozdev (2008) and Dimitrov et al. (2013). For instance, the estimated 100 years return level

for Ahtopol reported by these authors is 10.07m whereas the corresponding estimate given in Table 4 is 6.43m. Moreover, even the profile likelihood 95% upper confidence interval bound of 8.06 is lower than return value estimated by Grozdev (2008). We note that the results and findings of these authors are based on visual wave observations from the NIMH-BAS weather stations network and this may serve as an explanation of the distinction. Another reason of this underestimation might be due to the ECMWF reanalyses data usage such as ERA40, ERA-Interim and ERA-CLIM which tend to systematically underestimate the wind speeds in the Black Sea. As the hindcast data quality is a function of the wind fields this may lead to an underestimation of the wave hindcast data. Consequently, the statistical characteristics in the study are underestimated. Thus, the estimated return levels must be considered with caution and not directly taken into account in the decision making process with their numerical value but rather as a qualitative estimates or as lower limits of the return levels.

In this study only significant wave height data were considered. However, the wave period also plays important role in wave activity in the coastal zone. The study of incorporation of wave period data in the extreme value analysis of wave data will take place in our future activity.

More details about the performance of different reanalyses can be found in Van Vledder et al. (2015) and specifically for ERA-CLIM according to Galabov (2015a). Van Vledder et al. (2015) found that ECMWF ERA products including ERA-CLIM reanalyses underestimate wind speed in the Black Sea, while the most accurate wave hindcasts are those driven by the Climate forecast system reanalysis (CFSR) of the National Oceanic and Atmospheric Administration (NOAA). The new wave hindcast is planned to be done with SWAN model forced by CFSR reanalyses wind data. It should be noted that ERA-CLIM provides a long dataset spanning 1901-2010, while CFSR reanalyses are available after 1979. Therefore, the statistics obtained in this study based on the ERA-CLIM wave hindcasts is usefull information that can be used as a reference for the future extreme value analysis of significant wave height along the Bulgarian coast of the Black sea.

## REFERENCES

- Akpinar, A., van Vledder, G. P., Kömürçü, M. I., Özger, M. (2012). Evaluation of the numerical wave model (SWAN) for wave simulation in the Black Sea. *Continental Shelf Research*, vol. 50, pp. 80-99.
- Akpinar, A., Bingölbali, B. and Van Vledder, G. P. (2016). Wind and wave characteristics in the Black Sea based on the SWAN wave model forced with the CFSR winds. *Ocean Engineering*, vol. 126, pp. 276-298.
- Arkhipkin, V. S., Gippius, F. N., Koltermann, K. P. and Surkova, G. V. (2014). Wind waves in the Black Sea: results of a hindcast study. *Natural Hazards and Earth System Sciences*, vol. 14, pp. 2883-2897.

- Booij, N., Ris, R. C., and Holthuijsen, L. H. (1999). A third generation wave model for coastal regions: 1. Model description and validation. *Journal of geophysical research: Oceans*, vol. 104, pp. 7649-7666.
- Coles, S. (2001). *An introduction to statistical modeling of extreme values*. Springer, NY.
- Dimitrov D., Nyagolov I., Balabanova S., Lisev N., Koshinchanov G., Korcheva A., Marinski Y., Pashova L., Grozdev D., Vasilev V., Bozhilov and N. Tsvetkova. 2013. *Methods for assessment of flood hazard and flood risk, according to requirements of the EU Floods Directive 2007/60: Final Report, Black Sea Basin Directorate, Contract No D-30-62, 357 p.* (In Bulgarian). <http://www.moew.government.bg/?show=top&cid=67>.
- Embrechts, P., Klueppelberg, C., and Mikosch, T. (1997). *Modelling extremal events*. Springer.
- Galabov, V., Kortcheva, A. and Dimitrova, M. (2012). Towards a system for sea state forecasts in the Bulgarian Black Sea coastal zone: the case of the storm of 07-08 February 2012. *SGEM2012 Conference Proceedings/ ISSN 1314-2704, vol. 3, pp. 1017-1024*.
- Galabov, V. (2013). On the parameterization of white capping and wind input in deep and shallow waters and the strategies for nearshore wave modeling in closed seas. *Bulgarian Journal of Meteorology and Hydrology*, vol. 18, 1-2, pp. 18-38.
- Galabov, V. (2015a). The Black Sea Wave Energy: The Present State and the Twentieth century Changes. *arXiv preprint arXiv:1507.01187*.
- Galabov, V., Kortcheva, A., Bogatchev, A., Tsenova, B. (2015b). Investigation of the hydro-meteorological hazards along the Bulgarian coast of the Black Sea by reconstructions of historical storms. *Journal of Environmental Protection and Ecology*, vol. 16(3), pp. 1005-1015.
- Grozdev, D. (2008). Extreme characteristics of the Black Sea level along the Bulgarian coastline, In: *Proc. of Nat. Conf. with intern. participation GESCENCES'2008, BGS, Sofia, 125-126* (in Bulgarian).
- Komen, G. J., Hasselmann, S., and Hasselmann, K., (1984). On the existence of a fully developed wind sea spectrum. *Journal of Physical Oceanography*, vol. 14, pp. 1271-1285.
- R: A language and environment for statistical computing, R Development Core Team, R Foundation for Statistical Computing, Vienna, Austria, 2003, ISBN 3-900051-00-3, <http://www.R-project.org>
- Reiss, R.-D. and Thomas, M. (2007). *Statistical Analysis of Extreme Values: with Applications to Insurance, Finance, Hydrology and Other Fields*. 3<sup>rd</sup> ed., Birkhäuser, Basel.
- Stephenson, A. G. (2002) The ismev package. Reference manual: <http://CRAN.R-project.org/doc/packages/ismev.pdf>
- Stickler, A., Brönnimann, S., Valente, M. A., Bethke, J., Sterin, A., Jourdain, S., Roucaute, E., Vasquez, M.V., Reyes, D.A., Allan, R., Dee, D. (2014). ERA-CLIM: historical surface and upper-air data for future reanalyses. *Bulletin of the American Meteorological Society*, vol. 95, pp.1419-1430.
- Van Vledder, G. P., and Akpınar, A. (2015). Wave model predictions in the Black Sea: sensitivity to wind fields. *Applied Ocean Research*, vol. 53, pp. 161-178.
- Valchev, N., Davidan, I., Belberov, Z., Palazov, A., Valcheva, N., and Chin, D. (2010). Hindcasting and assessment of the western Black Sea wind and wave climate. *Journal of Environmental Protection and Ecology*, vol. 11, pp. 1001-1012.